

## Polarized-Proton Elastic Scattering from Polarized $^{13}\text{C}$

G. W. Hoffmann, M. L. Barlett,<sup>(a)</sup> W. Kielhorn, G. Pauletta,<sup>(b)</sup> M. Purcell, and L. Ray

*Department of Physics, The University of Texas, Austin, Texas 78712*

J. F. Amann, J. J. Jarmer, K. W. Jones, S. Penttilä, and N. Tanaka

*Los Alamos National Laboratory, Los Alamos, New Mexico 87545*

G. Bureson, J. Faucett,<sup>(c)</sup> M. Gilani, G. Kyle, and L. Stevens<sup>(d)</sup>

*Department of Physics, New Mexico State University, Las Cruces, New Mexico 88003*

A. M. Mack and D. Mihailidis

*Department of Physics, The University of Minnesota, Minneapolis, Minnesota 55455*

T. Averett, J. Comfort, J. Gorgen, and J. Tinsley

*Department of Physics, Arizona State University, Tempe, Arizona 85287*

B. C. Clark and S. Hama

*Department of Physics, The Ohio State University, Columbus, Ohio 43210*

R. L. Mercer

*IBM Watson Research Laboratories, Yorktown Heights, New York 10598*

(Received 4 September 1990)

The  $\vec{p} + {}^{13}\vec{\text{C}}$  (polarized target) elastic-scattering spin observables  $A_{00n}$  (target analyzing power) and  $A_{00nn}$  (spin-correlation parameter) were determined at 497.5 MeV over the laboratory angular range  $12^\circ$ – $30^\circ$  with statistical uncertainties typically  $\pm (0.02$ – $0.06)$ . Results of distorted-wave Born approximation calculations, based on either the relativistic or the nonrelativistic impulse approximation, are in reasonable agreement with these new data.

PACS numbers: 25.40.Cm, 24.10.Eq, 24.70.+s

The medium-energy proton-nucleus scattering data taken over the last twenty years for even-even target nuclei have stimulated calculations of density-dependent nucleon-nucleon ( $NN$ ) effective interactions from a few MeV to  $\sim 1$  GeV,<sup>1,2</sup> investigations of off-shell and full-folding effects in the proton-nucleus optical potential,<sup>3-5</sup> studies of ground-state matter densities<sup>6</sup> and matter transition densities for collective excitations,<sup>7</sup> and development of the relativistic impulse approximation (RIA), based on the Dirac equation.<sup>8-10</sup>

However, studies of elastic and inelastic (collective) scattering for  $J^\pi=0^+$  targets are sensitive mainly to just the no-spin and no-isospin transfer components of the  $NN$  interaction and the isoscalar, one-body densities of the target. Other types of reactions can be studied to investigate the spin and/or isospin transfer components of the  $NN$  interaction and the single-particle aspects of nuclear structure. These reactions include non-natural-parity inelastic excitations and charge-exchange processes. Another possibility<sup>11</sup> is proton elastic scattering from polarized, odd-mass nuclear targets. In this Letter we report the results of a medium-energy proton elastic-scattering experiment with a polarized  $^{13}\text{C}$  target: a measurement of the target analyzing power<sup>12</sup>  $A_{00n}$  and the spin-correlation parameter<sup>12</sup>  $A_{00nn}$  for  $E_p=497.5$  MeV.

Data were taken at the Clinton P. Anderson Meson Physics Facility (LAMPF) with the high-resolution spectrometer (HRS). The target nuclei,  $^{13}\text{C}$  and  $^1\text{H}$ , were polarized by using the dynamic nuclear polarization (DNP) technique.<sup>11,13,14</sup> The target material was 99-at.-%- $^{13}\text{C}$ -enriched ethylene glycol,  $^{13}\text{C}_2\text{H}_6\text{O}_2$ . Polarizing centers for DNP were created by doping the material with a paramagnetic complex<sup>15</sup> ( $7 \times 10^{19}$  molecules/cm<sup>3</sup>). The material was in the form of glassy beads about 1.5 mm in diameter contained in a 1-cm-diam thin-walled (0.13 mm) cylindrical Teflon cell (1.6 cm<sup>3</sup> in volume). The cylindrical axis of the target cell was parallel to the 2.5-T field of a C-type electromagnet with magnetic field oriented perpendicular to the scattering plane. The target was cooled to 0.5 K using a pumped  $^3\text{He}$  evaporation refrigerator. DNP occurs when the target is irradiated with microwaves of frequency near 69 GHz. The effective thicknesses of  $^{13}\text{C}$  and  $^1\text{H}$  were 280 and 66 mg/cm<sup>2</sup>, respectively. The overall energy resolution was typically 1 MeV (FWHM). A single coil provided both the  $^{13}\text{C}$  and  $^1\text{H}$  nuclear-magnetic-resonance (NMR) signals, which were used to determine the  $^{13}\text{C}$  and  $^1\text{H}$  polarizations for the entire target material.<sup>13</sup> The NMR measurements were calibrated by measuring the target thermal-equilibrium polarizations for both nuclei (no microwaves applied) near 1 K.

The hydrogen polarization of the target was also measured by using a target polarimeter which monitored  $\vec{p} + \vec{p}$  elastic scattering at  $\theta_{c.m.} = 46^\circ$ , and relied upon the known values of  $A_y = A_{00n}$  and  $A_{00nn}$  for 500-MeV  $\vec{p} + \vec{p}$ . The  $^1\text{H}$  and  $^{13}\text{C}$  polarizations are related through the equal-spin-temperature (EST) hypothesis:<sup>13,14</sup>

$$P = \tanh(\mu B / k_B T_s), \quad (1)$$

where  $P$  is the proton ( $^{13}\text{C}$ ) polarization,  $\mu$  is the proton ( $^{13}\text{C}$ ) magnetic moment,  $T_s$  is the spin temperature (assumed equal for  $^1\text{H}$  and  $^{13}\text{C}$ ),  $B$  is the field in which the dynamic cooling takes place, and  $k_B$  is the Boltzmann constant. The validity of the EST hypothesis for this target material was verified ( $\pm 2\%$ ) by comparing the NMR measurements for  $^{13}\text{C}$  and  $^1\text{H}$ , both before and after the target was irradiated by the beam protons. The target polarimeter and the EST hypothesis proved indispensable during the experiment in that they allowed the effects of beam-induced radiation damage to be directly determined and accounted for. Although the NMR and polarimeter results agreed within errors when the target material was fresh, differences grew with increased integrated beam flux through the target.<sup>14</sup> These differences are expected because the polarimeter monitors the beam-target interaction region (corresponding to a beam spot size of approximately 0.5 cm), while the NMR signal mainly comes from the outer portion of the target material closest to the NMR coil. During the course of the experiment, the target material was annealed<sup>14</sup> (7 times total) by raising its temperature to 180 K whenever the target polarization dropped to one-half of the value obtained immediately after annealing. Typical  $^{13}\text{C}$  polarization after annealing was 28%. The target material was also replaced once during the experiment. Beam polarization (normal to the scattering plane, and determined by quench-ratio measurements<sup>16</sup>) was reversed in direction every 2 min and was typically 80%. A beam-line polarimeter upstream of the target monitored the asymmetry in  $p + p$  elastic scattering at  $45^\circ$  c.m. using a thin  $\text{CH}_2$  foil and gave beam polarizations which were consistent with those from the quench-ratio measurements. Target polarization direction (normal to the scattering plane) was reversed approximately every 8–16 h by changing microwave frequency.

The target magnet deflected the beam to the left by  $18^\circ$ ; the magnet's center, and hence, the target's center, was offset  $\sim 0.5$  cm upstream and  $\sim 1$  cm beam left from the HRS pivot in order that the virtual object was in the position required by the HRS optics. The HRS was used to momentum analyze scattered protons and generate missing-mass spectra. Data were taken between laboratory angles  $12^\circ$  and  $30^\circ$  in about  $1.5^\circ$ – $2.0^\circ$  steps for the  $^{13}\text{C}$  target and also for an empty-target cell (to enable background corrections) and a thin, unpolarized  $^{13}\text{C}_2\text{H}_6\text{O}_2$  target (the ethylene glycol was sandwiched between two thin Be foils separated by 1 mm) to

allow accurate determination of the  $^{13}\text{C}/^{16}\text{O}$  cross-section ratios. The data from the dummy target and the thin  $^{13}\text{C}$  target were crucial to the experiment because the  $^{13}\text{C}$  and  $^{16}\text{O}$  elastic peaks were not well resolved except at the larger angles. See Fig. 6 of Ref. 17 for typical missing-mass spectra.

For beam and target polarizations normal to the scattering plane the yield at a particular scattering angle is given by

$$Y = \sigma_0 \left( \frac{N_A \rho t}{A} \right) [1 + P_b A_{00n0} + P_t A_{000n} + P_b P_t A_{00nn}] I_0 \Delta \Omega \epsilon, \quad (2)$$

where  $\sigma_0$  is the unpolarized differential cross section,  $N_A \rho t / A$  is the number of target nuclei per unit area,  $P_b$  and  $P_t$  are the appropriate (average) beam and target polarizations (either positive or negative),  $A_{00n0} \equiv A_y$  is the projectile analyzing power,  $A_{000n}$  is the target analyzing power, and  $A_{00nn}$  is the spin-correlation parameter.<sup>12</sup> The quantities  $I_0$ ,  $\Delta \Omega$ , and  $\epsilon$  are the incident number of beam protons, the HRS solid angle, and overall efficiency, respectively. The subscript  $n$  refers to the direction  $\hat{n}$ , where  $\hat{n} = (\mathbf{k} \times \mathbf{k}') / |\mathbf{k} \times \mathbf{k}'|$ ,  $\mathbf{k}$  ( $\mathbf{k}'$ ) being the initial (final) proton-nucleus relative momentum in the center-of-momentum (c.m.) system. Yields were obtained at each angle for each of the four beam-target polarization directions ("up-up," "down-up," etc.).  $A_{000n}$  and  $A_{00nn}$  were obtained from these equations after subtracting background and  $^{16}\text{O}$  contributions as determined by the information from the empty-target and thin-target runs. Small differences ( $\leq 1\%$ ) in effective target thickness between runs in which the target polarization was "up" and "down" (due to the cylindrical target geometry and the composition of the target material which consisted of irregularly packed frozen beads) had to be determined carefully to avoid large, systematic errors in the deduced analyzing powers. A parameter  $C$  was introduced and fixed such that the difference,  $(Y'_{\uparrow\uparrow} + Y'_{\downarrow\uparrow}) - C(Y'_{\uparrow\downarrow} + Y'_{\downarrow\downarrow})$ , vanished in the elastic region of the yield spectrum for nuclei with  $A > 13$ :  $^{16}\text{O}$ , Cr, Cu, F, and other material in the target region (i.e., no  $^{13}\text{C}$  yield). Here  $Y'_{\uparrow\downarrow}$  denotes a normalized yield [i.e.,  $Y/I_0\epsilon$ , see Eq. (2)] for beam polarization up, target polarization down, etc., and the parameter  $C$  depends upon effective target thicknesses for target polarization up and down runs as well as upon small differences in beam polarization magnitudes for the various beam-target polarization combinations.  $C$  varied over the range 0.97–1.10, and its statistical uncertainty was a major contributor to the errors in the deduced analyzing powers [typically a  $\pm(0.01$ – $0.05)$  contribution].

The results for  $A_{000n}$  and  $A_{00nn}$  are shown in Fig. 1 along with theoretical predictions. The errors shown account for all sources of statistical uncertainty; the statistics of the measured yields account for essentially all of

the uncertainty. Systematic errors in the beam and target polarizations, as well as those associated with the HRS data-acquisition system, are estimated to be negligible. Both data sets are smooth with respect to their angular distributions and display structure in the angular regions near the minima in the differential cross section ( $18.5^\circ$  and  $34.5^\circ$  in the c.m. system) as expected. The complete data set for polarized proton elastic scattering from unpolarized  $^{13}\text{C}$  at 500 MeV was reported in Ref. 18.

The theoretical results for  $A_{000n}$  and  $A_{00nn}$  shown in Fig. 1 were computed in the distorted-wave Born approximation (DWBA) for both the relativistic impulse-approximation (RIA) model<sup>19</sup> and the nonrelativistic impulse-approximation (NRIA) model. For both calculations the  $^{13}\text{C}$  wave function was assumed to be a pure  $1p_{1/2}$  neutron single-particle state coupled to an inert  $^{12}\text{C}$  "core," and the scattering amplitude, corresponding to the twelve-nucleon core, was obtained from a Dirac-phenomenological-optical-model fit to the 500-MeV  $\bar{p}+^{12}\text{C}$  elastic-scattering data.<sup>18</sup> The  $NN$   $t$  matrices (in both the RIA and NRIA forms) in the proton-nucleus Breit frame were generated from the SP82  $NN$  phase-shift solution<sup>20</sup> by using the transformation developed in Ref. 10.

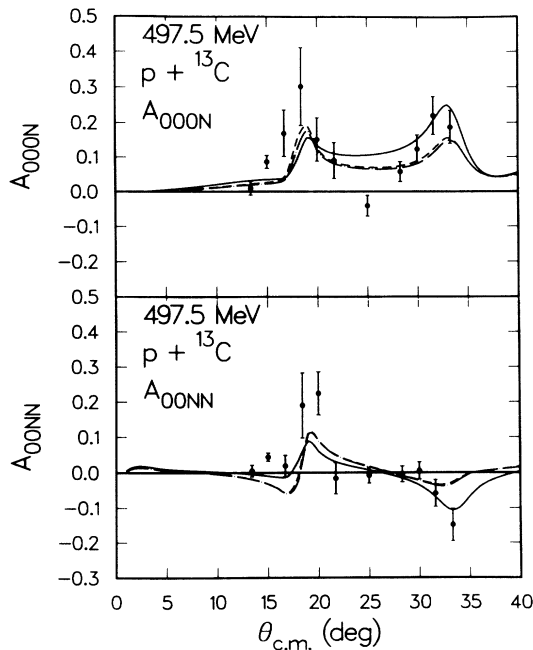


FIG. 1. Experimental data and theoretical predictions for  $\bar{p}+^{13}\text{C}$  target spin observables  $A_{000n}$  (upper portion) and  $A_{00nn}$  (lower portion) at 497.5 MeV as discussed in the text. Errors in the data include all statistical sources of uncertainty. The RIA-DWBA predictions assuming the relativistic mean-field (nonrelativistic) value for the valence neutron lower-component wave function are indicated by the solid (dashed) curves. The NRIA-DWBA predictions are given by the dash-dotted curves.

For the RIA-DWBA calculations the  $NN$  Lorentz-invariant amplitudes were assumed to be given by the local form<sup>21</sup>

$$F = F_S + F_P \gamma_1^5 \gamma_2^5 + F_V \gamma_1^\mu \gamma_{2\mu} + F_A \gamma_1^5 \gamma_1^\mu \gamma_2^5 \gamma_{2\mu} + F_T \sigma_1^\mu \sigma_{2\mu} \quad (3)$$

The valence neutron wave function was taken to be the  $1p_{1/2}$  eigenstate of the relativistic mean-field (RMF) scalar and timelike vector binding potentials for  $^{12}\text{C}$ .<sup>22</sup> The relativistic distorted waves were obtained through solution of the Dirac equation for  $\bar{p}+^{12}\text{C}$  elastic scattering by using the Dirac-phenomenological-optical potential.<sup>18</sup> The results are indicated in the figure by the solid curves. RIA-DWBA calculations were also done in which the relativistic enhancement of the lower component of the  $1p_{1/2}$  valence neutron wave function was suppressed, thus reducing its strength to the nonrelativistic limit.<sup>19</sup> These results are shown by the dashed curves. Other calculations were made with a pseudovector, rather than pseudoscalar, form for the  $NN$ -invariant amplitude,<sup>19</sup> and with the twelve-nucleon core contribution to the isoscalar, three-vector current.<sup>19</sup> Both of these results lie between the solid and dashed curves in the figure.

For the NRIA-DWBA calculations the full  $NN$   $t$  matrix in the proton-nucleus Breit frame was used.<sup>10</sup> This  $t$  matrix is given by

$$t_{NN} = t^a + t^b \sigma_{1n} \sigma_{2n} + t^c \sigma_{1n} + t^c \sigma_{2n} + t^d \sigma_{1q} \sigma_{2q} + t^e \sigma_{1p} \sigma_{2p}, \quad (4)$$

where  $\sigma_{1x} \equiv \sigma_1 \cdot \hat{x}$ ,  $\hat{n} = (\mathbf{k} \times \mathbf{k}') / |\mathbf{k} \times \mathbf{k}'|$ ,  $\hat{q} = (\mathbf{k} - \mathbf{k}') / |\mathbf{k} - \mathbf{k}'|$ , and  $\hat{p} = (\mathbf{k} + \mathbf{k}') / |\mathbf{k} + \mathbf{k}'|$ . Direct and exchange contributions were included, and the amplitudes  $t^a$  through  $t^e$  were taken to be functions of momentum transfer only. The NR distorted waves were generated by solving the Schrödinger equation with relativistic kinematics by using the Schrödinger equivalent potential<sup>23</sup> of the Dirac-phenomenological-optical potential for  $\bar{p}+^{12}\text{C}$ . The valence neutron wave function was assumed to be the (properly normalized) upper component of the RMF  $1p_{1/2}$  eigenstate. The NRIA-DWBA predictions are shown by the dash-dotted curves in the figure.

Each of the calculations qualitatively describes the data for both observables, although all are lacking in necessary structure in the region from  $15^\circ$  to  $25^\circ$  c.m. Compared to the discrepancies between theory and data, the differences between the two RIA-DWBA predictions are small as are the differences between the RIA- and NRIA-DWBA predictions. Results using the SP89 phase-shift solution are very similar to those presented here, and these and other results based on density-dependent effective interactions and more realistic nuclear-structure input will be discussed in a later article. Nonrelativistic-Glauber-model predictions<sup>24</sup> for  $A_{000n}$  are in poor agreement with these data.

In summary, there are a variety of motivations for doing medium-energy scattering experiments for polarized protons on polarized nuclear targets. These primarily involve studies of the  $NN$  effective interaction and relativistic effects. The results reported here for  $\bar{p} + {}^{13}\text{C}$  at 500 MeV show that such experiments are difficult, but possible, and that quality data can be obtained. These new types of scattering data are qualitatively explained by current theoretical models, but further improvements will evidently be necessary before quantitative understanding can be achieved. Other DNP polarized targets are being developed that will lead to a new generation of experiments that in turn will provide much higher-quality data and impose more stringent tests on the reaction models.

This work was supported in part by the U.S. Department of Energy, the Robert A. Welch Foundation, and the National Science Foundation. The authors wish to thank the Los Alamos National Laboratory and the LAMPF Director, G. T. Garvey, in particular, for encouragement and support of this experiment.

<sup>(a)</sup>Present address: Applied Research Laboratories, The University of Texas, Austin, TX 78713.

<sup>(b)</sup>Present address: Department of Physics, University of Udine, 33100 Udine, Udine, Italy.

<sup>(c)</sup>Present address: Los Alamos National Laboratory, Los Alamos, NM 87545.

<sup>(d)</sup>Present address: Department of Physics, Arizona State University, Tempe, AZ 85287.

<sup>1</sup>L. Rikus and H. V. von Geramb, Nucl. Phys. A **426**, 496 (1984).

<sup>2</sup>L. Ray, Phys. Rev. C **41**, 2816 (1990).

<sup>3</sup>Ch. Elster, T. Cheon, E. F. Redish, and P. C. Tandy, Phys. Rev. C **41**, 814 (1990).

<sup>4</sup>H. F. Arellano, F. A. Brieva, and W. G. Love, Phys. Rev. C **41**, 2188 (1990).

<sup>5</sup>R. Crespo, R. C. Johnson, and J. A. Tostevin, Phys. Rev. C **41**, 2257 (1990).

<sup>6</sup>L. Ray, Phys. Rev. C **19**, 1855 (1979).

<sup>7</sup>J. J. Kelly *et al.*, Phys. Rev. C **41**, 2504 (1990).

<sup>8</sup>J. A. McNeil, J. Shepard, and S. J. Wallace, Phys. Rev. Lett. **50**, 1439 (1983); **50**, 1443 (1983).

<sup>9</sup>B. C. Clark, S. Hama, R. L. Mercer, L. Ray, and B. D. Serot, Phys. Rev. Lett. **50**, 1644 (1983).

<sup>10</sup>L. Ray and G. W. Hoffmann, Phys. Rev. C **31**, 538 (1985).

<sup>11</sup>*Proceedings of the LAMPF Workshop on Physics with Polarized Nuclear Targets*, Los Alamos National Laboratory, edited by G. Burleson, W. Gibbs, G. Hoffmann, J. J. Jarmer, and N. Tanaka (LAMPF Conference Report No. LA-10772-C, 1986).

<sup>12</sup>The notation for both the  $NN$  and  $p + {}^{13}\text{C}$  spin observables is that of J. Bystricky, F. Lehar, and P. Winternitz, J. Phys. (Paris) **39**, 1 (1978).

<sup>13</sup>J. J. Jarmer, S. Penttilä, D. Hill, T. Kasprzyk, M. Krumploc, M. L. Barlett, G. W. Hoffmann, and L. Ray, Nucl. Instrum. Methods Phys. Res., Sect. A **250**, 576 (1986); D. Hill, T. Kasprzyk, J. J. Jarmer, S. Penttilä, M. Krumploc, G. W. Hoffmann, and M. Purcell, Nucl. Instrum. Methods Phys. Res., Sect. A **277**, 319 (1989).

<sup>14</sup>S. I. Penttilä, J. F. Amann, J. J. Jarmer, K. W. Jones, N. Tanaka, M. L. Barlett, G. W. Hoffmann, W. F. Kielhorn, G. Pauletta, and M. Purcell, in *High-Energy Spin Physics*, edited by K. J. Heller, Particles and Fields Series No. 37, AIP Conference Proceedings No. 187 (American Institute of Physics, New York, 1989), p. 1281.

<sup>15</sup>The chemical dopant was sodium bis(2-ethyl-2-hydroxybutyrate)-oxochromate(V) monohydrate, commonly known as EHBA-Cr(V).

<sup>16</sup>M. W. McNaughton, P. R. Bevington, H. B. Willard, E. Winkelmann, E. P. Chamberlin, F. H. Cverna, N. S. P. King, and H. Willmes, Phys. Rev. C **23**, 1128 (1981).

<sup>17</sup>G. W. Hoffmann, in *Physics with Polarized Beams on Polarized Targets*, edited by J. Sowinski and S. E. Vigdor (World Scientific, Singapore, 1990), p. 139.

<sup>18</sup>G. W. Hoffmann *et al.*, Phys. Rev. C **41**, 1651 (1990).

<sup>19</sup>L. Ray, G. W. Hoffmann, M. L. Barlett, J. D. Lumpe, B. C. Clark, S. Hama, and R. L. Mercer, Phys. Rev. C **37**, 1169 (1988).

<sup>20</sup>R. A. Arndt, L. D. Roper, R. A. Bryan, R. B. Clark, B. J. VerWest, and P. Signell, Phys. Rev. D **28**, 97 (1983).

<sup>21</sup>J. A. McNeil, L. Ray, and S. J. Wallace, Phys. Rev. C **27**, 2123 (1983).

<sup>22</sup>C. J. Horowitz and B. D. Serot, Nucl. Phys. A **368**, 503 (1981); B. D. Serot (private communication).

<sup>23</sup>B. C. Clark, in *Medium Energy Nucleon and Antinucleon Scattering*, edited by H. V. von Geramb, Lecture Notes in Physics Vol. 243 (Springer-Verlag, Berlin, 1985), p. 391.

<sup>24</sup>I. N. Kudryavtsev and A. P. Soznik, J. Phys. G **15**, 1377 (1989).